CHARACTERISTICS OF WHITECAPS ESTIMATED FROM IMAGE PROCESSING OF THE OCEAN SURFACE

YUKUN WANG
Kyushu University, Kasuga, Fukuoka, Japan, ou@esst.kyushu-u.ac.jp

RYO OHNISHI
Kyushu University, Kasuga, Fukuoka, Japan, oonishi@esst.kyushu-u.ac.jp

YUJI SUGIHARA
Kyushu University, Kasuga, Fukuoka, Japan, sugihara.yuji.290@m.kyushu-u.ac.jp

YOSHIHIRO NAKAMURA
Kyushu University, Kasuga, Fukuoka, Japan, nakamura@esst.kyushu-u.ac.jp

OSAMA ELJAMAL
Kyushu University, Kasuga, Fukuoka, Japan, osama-eljamal@kyudai.jp

ABSTRACT

Whitecaps generated by wave breaking on the ocean surface play an important role in the local interaction between the atmosphere and the ocean. Whitecap coverage is defined by the area of whitecaps per the unit ocean surface. It has been recognized as one of important physical quantities for describing the ocean surface fluxes such as the momentum, heat and carbon dioxide, so that the quantitative evaluation of whitecap coverage becomes significant from viewpoints of environmental hydraulics and ocean engineering. In this study, in order to validate typical estimation methods for whitecap coverage, the AWE algorithm proposed by Callaghan and White (2008) was compared with the threshold method adopted usually in previous studies. The agreement between both was examined on the basis of the influence of solar radiation. Previous studies have suggested that the depth of bubble penetration generated by wave breaking may be proportional to the significant wave height. Based on this assumption, we proposed a new index for expressing characteristics of whitecaps, i.e., whitecap depth, indicating the product of whitecap coverage and the bubble penetration depth. This quantity denotes the averaged depth of the bubbly layer per the unit ocean area, and can be expected to become a more significant quantity than whitecap coverage. In addition, for the data of whitecap coverage obtained from the AWE method, we investigated the relation of whitecap depth with 10-m wind speed or the windsea Reynolds number.

Keywords: *Whitecap coverage, Wave breaking, Image processing, AWE, Whitecap depth*

1. INTRODUCTION

Whitecaps play an important role in the exchange processes of the momentum, heat and gas between the atmosphere and the ocean because turbulence and bubbles are generated during its formation. In order to predict the concentration of CO_2 in the atmosphere in the future, it is important to clarify the mechanism of gas transfer into the ocean with huge carbon storage. Whitecap coverage W_c is one of quantitative indicators for the whitecapping ocean surface, and it is also an important parameter for calculating the CO_2 exchange rate between the atmosphere and the ocean. W_c is defined as the ratio of whitecapping area per the unit area of the ocean surface, which is well-known to be highly correlated with the wind speed above the ocean surface. Whitecap coverage is usually expressed as a function of the wind speed U or the friction velocity u_*, whose typical functions are $W_c=aU^b$ and $W_c=au_*^b$, where a and b stand for empirical constants. Previous studies on the dependence of whitecaps on the wind speed began around 1950, and as an example, Munk (1947) reported that whitecaps become active at the wind speed of 6m/s or higher. In addition, Gathman and Trent (1968) pointed out that whitecaps are unlikely to occur when the wind speed is less than 3m/s.

Monahan (1971) used camera images of the ocean surface taken by ships at 71 observation points in the Atlantic Ocean to separate whitecapping area and the other one, and measured their weight ratios to estimate whitecap coverage. In addition, the average weight ratio of 5 to 20 images was used as the average whitecap coverage from 30 minutes to 1 hour, and the following empirical formula was proposed:

$$W_c = 1.35 \times 10^{-4} {U_{10}}^{3.4}. \quad (1)$$

Here, U_{10} (m/s) represents the average wind speed at 10m above the sea surface. In addition, based on the similar methods, Monahan and Cardone (1970), Toba and Chaen (1973), and Wu (1979) proposed empirical

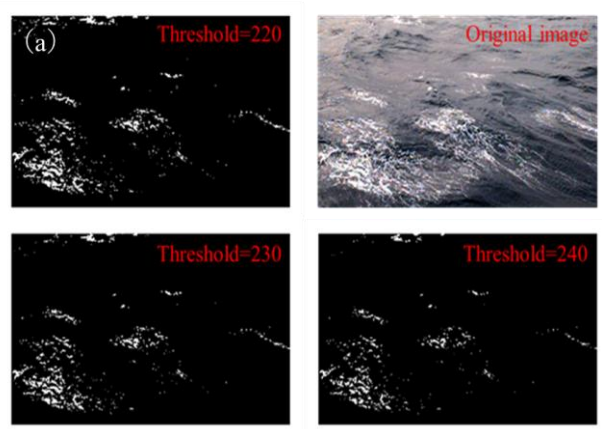

Figure 1. Comparison between original and binary images

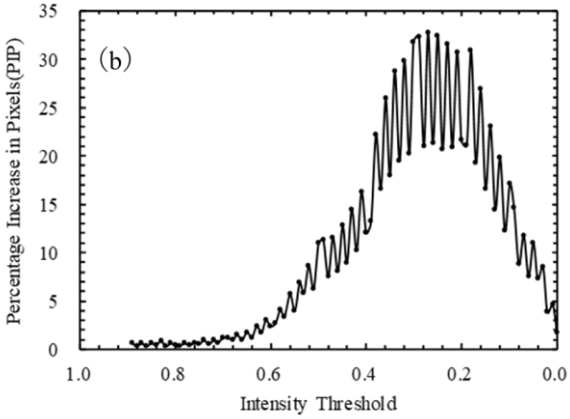

Figure 2. Change of PIP for each intensity threshold

relations for whitecap coverage. Monahan (1993) identified whitecap breakers by converting original sea surface images into 256-level grayscale images and setting luminance thresholds. From such an image analysis, he found that there is a relationship between whitecap coverage and the cubic power of wind speed as the following relation:

$$W_c = c_1(U_{10} - c_0)^3, \tag{2}$$

where c_1 and c_0 denote empirical constants. Though the above relation is an empirical one, but it is widely supported by many other researchers (e.g., Asher and Wanninkhof (1998), Asher et al. (2002), Stramska and Petelski (2003)).

In addition, Sugihara et al. (2007) evaluated the long-term whitecap coverage by applying a certain constant threshold to all of the ocean surface images taken at a sea observation tower. However, the brightness of the ocean surface varies largely according to the weather and the viewing angle of the video camera, so that it is desire to set the most suitable threshold for the respective images.

As one of the methods to solve this problem, Callaghan and White (2008) proposed an image processing method called the automatic whitecap extraction (AWE). AWE is an algorithm based on a linear differential analysis for the brightness data, and estimates automatically the most suitable threshold for the respective images, and it can divide the ocean surface image structure called PIP (percentage of pixel increase) into the region A (whitecap-breaking), the region B (ocean surface with high brightness) and the region C (normal ocean surface). Their method may useful to identify the boundary between regions A and B, and estimate the threshold for each image independent of subjectively-determined threshold and the change in lighting environments caused by the weather. However, the validation of AWE in their study seems to be insufficient, and the applicability of AWE in long-term ocean observation has not been clarified yet.

Thorpe (1986) and Yoshioka (2003) investigated the bubbly layer depth due to wave breaking. This is the depth at which bubbles penetrate when whitecaps rush into the water, which was reported to be about 5 times the significant wave height. The bubble penetration depth is also expected to be one of the important factors for quantifying the exchange process of CO_2 instead of the coverage of whitecaps.

In this study, the method of AWE proposed by Callaghan and White (2008) was compared with the threshold method adopted usually in previous studies. The agreement between both was examined on the basis of the influence of solar radiation. In addition, we proposed a new index for expressing characteristics of whitecaps, i.e., whitecap depth, indicating the product of whitecap coverage and the bubble penetration depth.

2. OBSERVATION METHOD

The data used in this study were taken at a sea observation tower in Tanabe Bay (Shirahama Oceanographic Observatory, Kyoto University), Shirahama, Wakayama Prefecture, Japan. The observation tower faces the open seas in the southwest, and the average water depth around the tower is about 30m, but the observation tower is located on the reef at the depth of 9m. Since the size of the reef is relatively small, so that the influence of the topography of the seafloor on waves is almost negligible. At the observation tower, the air and water temperatures, air pressure and the other meteorological information, as well as the regular observations of the wave height and frequency. In this study, we used the wind speed at 12.5m above the sea level as U, the wind direction as WD, and the friction velocity as u_*. The sea surface images must be taken all the time in this study, and the camera used to take the image data was a WEB camera system with the resolution of 640x480 pixels. The camera was located at an altitude of 14m and at a dip angle of about 45°. The imaging time was 65 days from 29th January 2007 to 4th April 2007, and the images of 12 hours of daylight saving time from 6:00:00 to 17:59:50 were analyzed.

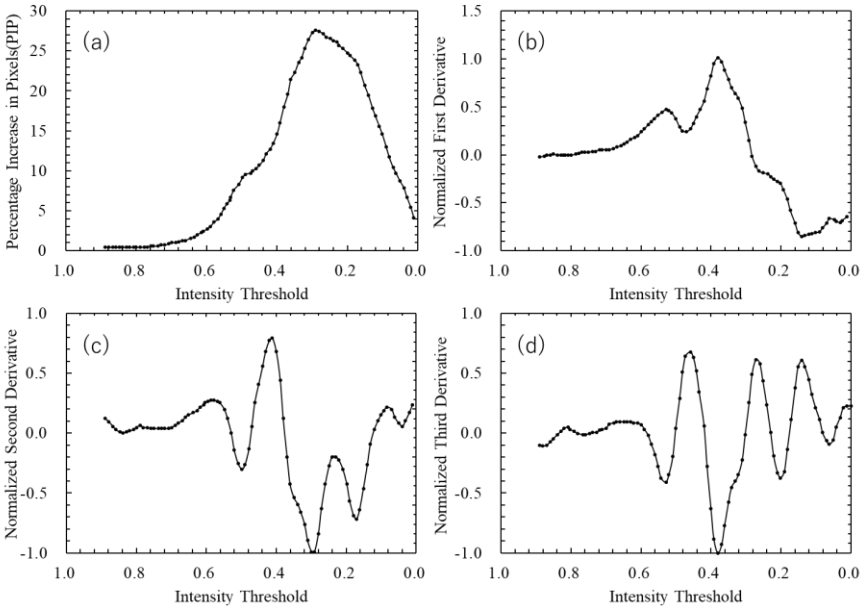

Figure 3. Analytical results based on AWE algorithm.

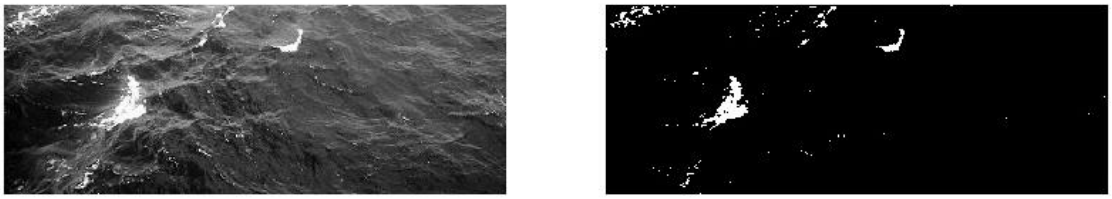

Figure 4. Whitecaps extracted based on AWE algorithm

3. DATA ANALYSIS

Since the reflected light has negative effects on the recognition of whitecapping region, these effects must first be eliminated by limiting the analysis area of the image. In this study, the analysis area was set to a certain region of 640 × 240 pixels on the sea surface image. After limiting the analysis area, the RGB scale image was converted to the grayscale image. Next, a threshold for distinguishing the grayscale sea surface image into a whitecap region and a non-whitecap one was determined. The image was binarized by using the value of the determined threshold, and then the whitecap and non-whitecap regions were identified. Finally, the area of the identified whitecap region was divided by the area of the whole analytical region, and we obtained the value of whitecap coverage.

As shown in Fig. 1, by using a conventional method for determining the threshold, we examine the binary image with respect to each threshold, and determine a better threshold through confirming the reproducibility of the distribution of the actual whitecap breakers. Mizuno (2008) calculated whitecap coverage by using a constant threshold of 230; thus we then call the Fixed Threshold method. This method is simple, but it may be inadequate because smaller values of whitecap coverage are estimated when a certain large threshold is applied.

Automatic whitecap extraction (AWE) is an algorithm proposed by Callaghan and White (2008) to automatically determine the coverage of whitecap, which does not need to determine a subjective threshold by researcher. One of the characteristics of AWE is to analyze pixel values with respect to each image to be analyzed and to determine the respective thresholds. This is very different from the traditional estimation such as the Fixed Threshold method. By setting a suitable threshold for each sea image, we can prevent the error by detecting non-whitecap region, and can calculate the value of whitecap coverage more accurately. In order to determine the threshold for AWE, PIP (percentage increase in the number of pixels) and the image structure must be used, where PIP is defined as follows:

$$\mathrm{PIP(i)} = \frac{P(i) - P(i + 0.01)}{P(i)} \times 100 \tag{3}$$

Here, P (i) represents the number of pixels for which the luminance value exceeds the value for i, and it has been calculated by changing the value of i from the maximum luminance value to the minimum one on the image step by step at a rate of 0.01. As an example of the analytical results, Fig. 2 shows the variation of PIP with the intensity threshold on the ocean surface image. It can be seen that the PIP for the ocean surface image becomes relatively constant in the high luminance band, i.e., the large values of the intensity threshold. Also,

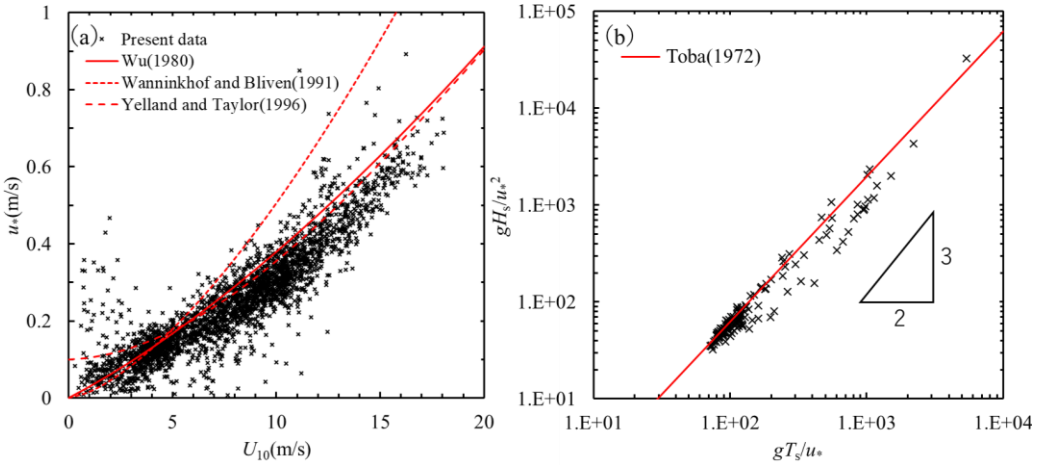

Figure 5. Meteorological and sea-state conditions: (a) Relation between U_{10} and u_* and (b) Relation between H_s and T_s

the value of PIP increases in the middle band, whereas it decreases in the lower band. Next, the differential analysis for PIP is used to determine the threshold to identify whitecaps located between the region A and the region B. In this study, since the PIP fluctuated greatly as shown in Fig. 2, the results have been smoothed by the four-point moving average to make the derivatives of PIP. The derivative equation is given by

$$\frac{d[\Phi(i)]}{di} = \frac{\Phi(i) - \Phi(i + \Delta i)}{\Delta i} \tag{4}$$

where i is the intensity threshold, and Δi is 0.01. Φ denotes PIP and its first and second derivatives. After the first derivative of PIP was calculated, it was smoothed again by the four-point moving average, and then Eq. (4) is used again for the second derivative. In addition, after smoothing in the same way, the third-order differential is performed. An example of a series of the processes is provided in Fig.3. The AWE algorithm increases the threshold from the minimum luminance value to the maximum luminance one, and identifies a zero crossing point where the negative value changes first to the positive one. This point represents the transition from region C to region B. In Fig. 3(b), it can be confirmed that the threshold exists between 0.28 and 0.29. Thus, the threshold of 0.28 is set as the lower threshold for subsequent processing. In addition, the maximum value of the first derivative is obtained from the zero crossing for the second derivative. The local maximum has the characteristic that it is almost located in the middle of region B. Figure 3(c) demonstrates the analytical results for the second derivative, and Fig. 3(d) also shows those for the third derivative. Finally, the average value of the inflection point from the low luminance band to the high luminance one is determined as the image threshold. The result of whitecaps extracted based on the AWE algorithm is shown in Fig. 4.

4. RESULTS AND DISCUSSION

Figure 5(a) shows the relationship between U_{10} and u_* during the observation period, where the empirical expressions of Wu (1980), Wanninkhof and Bliven (1991), and Yelland and Taylor (1996) are also shown for the comparison with the observation data. It is seen from this figure that u_* increases nonlinearly with the increase of U_{10}, which looks similar to the empirical relations of Wu(1980), and Yelland and Taylor (1996). Though the data dispersion is observed between U_{10} and u_* in this study, they almost match the behavior in the previous studies.

Figure 5(b) shows the relations between the significant wave height H_s and the significant wave period T_s obtained from the observed results. The solid line in the figure indicates the 3/2 power law, which is a statistical similarity law based on the local balance between wind and wind waves, and the law is given by the following relation:

$$\frac{gH_s}{u_*^2} = 0.062\left(\frac{gT_s}{u_*}\right)^{\frac{3}{2}} \tag{5}$$

Here, T_s has been calculated according to $T_s = T_p/1.05$ in this study. The coefficient of 0.062 is an empirical constant, which fluctuates about ±20% depending on the fluctuation of wind. According to Fig. 5(b), we exclude the ineffective whitecap data in comparison with Toba's 3/2 power law. Figure 6 shows the relations of Wc_AWE and Wc _FT with 10-m wind speed U_{10}, respectively. In the figures, both of Wc_AWE and Wc _FT

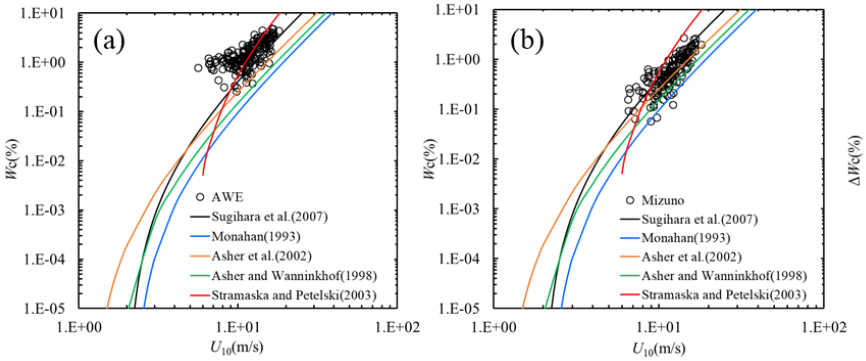

Figure 6. Relations of W_c_AWE and W_c _FT with U_{10}

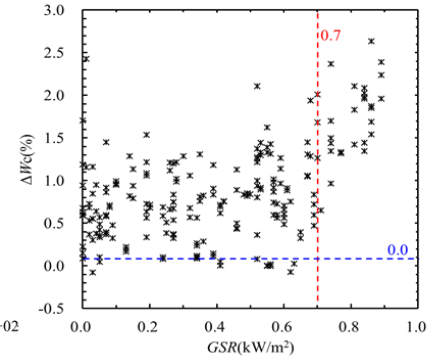

Figure 7. Relation between ΔW_c and GSR

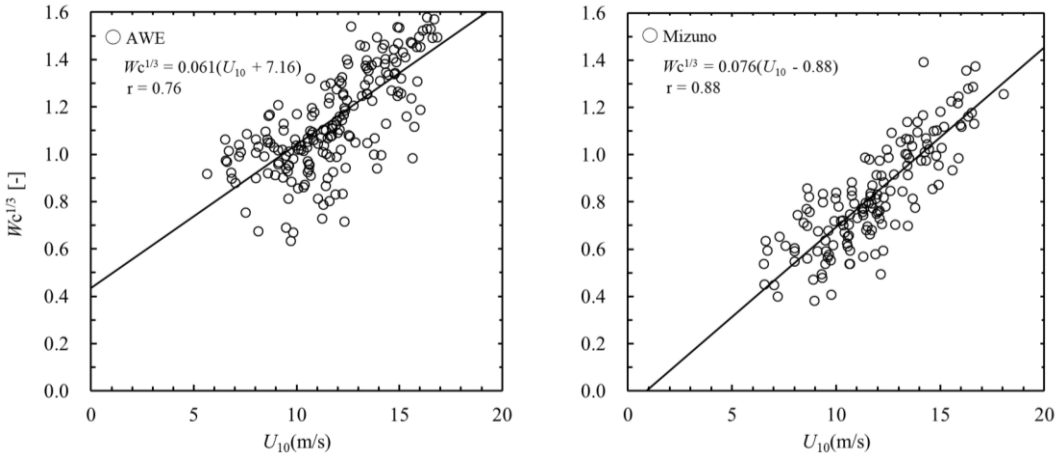

Figure 8. Relations of $W_c^{1/3}$ from AWE and FT with U_{10}

in addition to U_{10} are plotted as 20-minute averages. The data obtained by Mizuno (2008) are shown as Wc _FT in this study. He calculated W_c by fixing the brightness threshold of the ocean surface image at 230, and investigated the correlation of whitecap coverage with the meteorological and sea-state conditions. It is seen from Fig. 6 that when 10-m wind speed becomes 5m/s or higher, W_c _FT is in good agreement with the empirical relations of Monahan (1993) and Sugihara et al. (2007). The value of W_c_AWE is larger than their relations, but indicating high consistency with the relation of Stramaska and Petelski (2003). The value of W_c_AWE calculated in this study is significantly larger than that of W_c _FT, because W_c _FT sets the threshold at 230 to calculate whitecap coverage, which is larger than 175 of Sugihara et al. (2007) with the same manner, and thus W_c _FT makes the value of whitecap coverage underrated.

In Fig. 7, ΔW as the difference between Wc _FT and Wc _AWE is compared with the amount of the solar radiation GSR. When GSR exceeds about 0.7 kW/m^2, the value of ΔW is increase considerably. It is seen that due to the influence of solar radiation, it is usually difficult to calculate whitecap coverage under the condition of strong sunlight. Therefore, in order to investigate properly the behavior of whitecap coverage, we should exclude the data of whitecap coverage when the solar radiation exceeded 0.7 kW/m^2.

Figure 8 shows the relations between $W_c^{1/3}$ and U_{10} for W_c_AWE and W_c _FT. In addition, the linear regressions obtained by the least square method are also provided for both. In this study, the correlation coefficients of W_c_AWE and W_c _FT are 0.88 and 0.76, respectively. The data dispersion of W_c_AWE is greater than that of W_c _FT, indicating a lower correlation than W_c _FT. This is because the threshold of W_c _FT has been fixed at a higher value of 230, while the AWE algorithm does not have a fixed threshold range, so the dispersion of whitecap coverage data becomes larger. However, this does not mean that the accuracy of AWE algorithm becomes lower than that of fixed threshold algorithm.

In this study, we propose a new characteristic quantity of wave breaking, which is different from the traditional coverage of whitecap. Whitecap coverage is concerned with planar information on whitecaps on the ocean surface. However, in practice, whitecapping waves bring bubbles into a deeper layer of the sea, and thus it is impossible to quantify three-dimensional characteristics of whitecaps from the value of whitecap coverage. Therefore, considering the depth of the bubble penetration, we design three-dimensional characteristics of whitecaps, instead of two-dimensional information such as the coverage of whitecap. For this reason, we should first consider the penetration depth of bubbles formed by wave breaking.

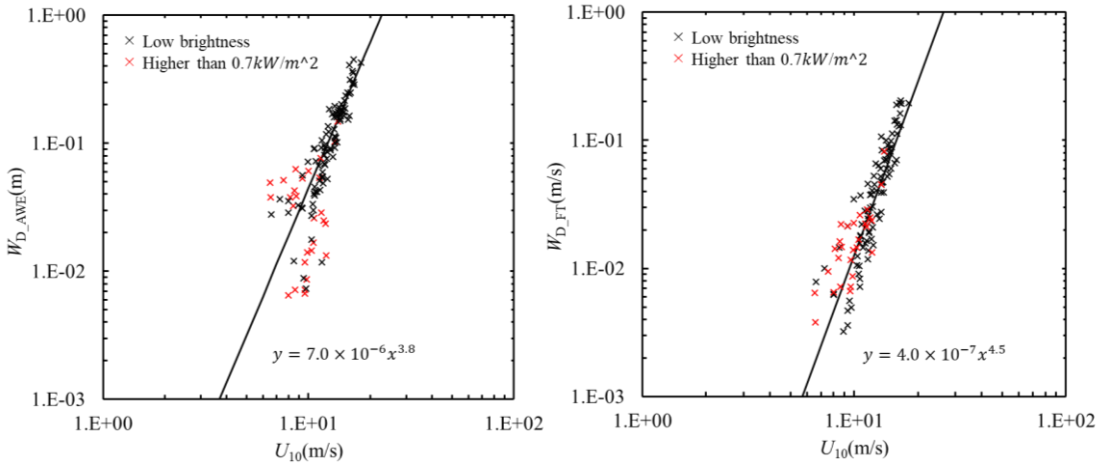

Figure 9. Relationships between W_D_AWE, W_D_FT and U_{10}

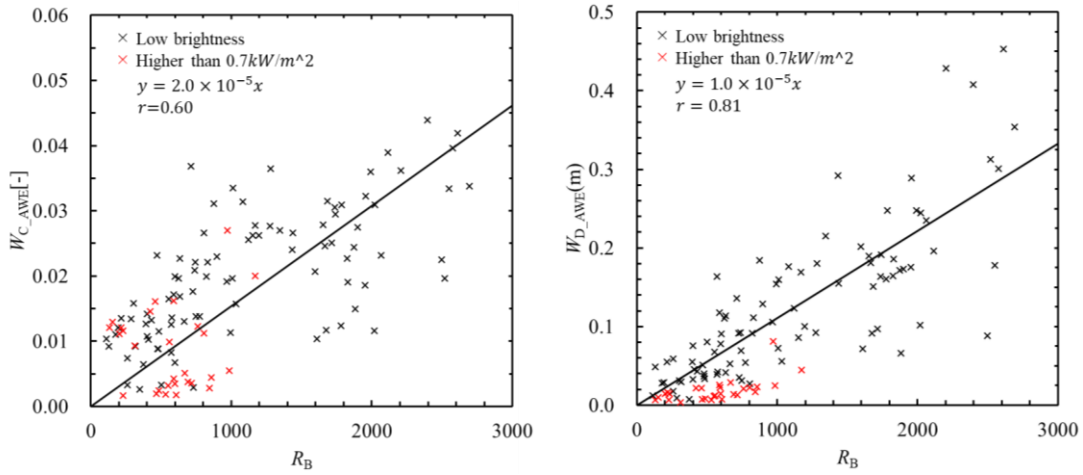

Figure 10. Relationships between W_c_AWE, W_D_AWE and R_B

Thorpe (1986) and Yoshioka et al. (2003) used the reflection intensity of sound beams in the ocean surface boundary layer to visualize the vertical distribution of bubbles underneath the ocean surface. Their observations demonstrated that the depth of bubbles generated by wave breaking becomes about 4 to 5 times of the significant wave height H_s. Based on the findings, the product of whitecap coverage W_c and the bubble penetration depth will be useful for expressing three-dimensional characteristics of the bubbly region of whitecaps. In this study, we propose a new characteristic quantity as whitecap depth W_D, which is defined as follows:

$$W_D = 5WH_s \tag{6}$$

This quantity denotes the averaged depth of the bubbly layer per the unit ocean area, and it is considered to be a more suitable index to evaluate characteristics of breaking waves than whitecap coverage. Figure 9 shows the relations of W_D_AWE and W_D_FT with U_{10}, both of which show a strong linear correlation, suggesting that W_D is recognized as a suitable quantity that can evaluate whitecaps more accurately than whitecap coverage.

The momentum transfer mechanism at the wind-wave interface is controlled by the turbulent fields closely connected with wave breaking, which depends on the wind speed and wave conditions. Some previous studies have investigated the transition process of the surface of wind waves. A typical outcome is the work of Toba and Koga (1986), and they proposed that a dimensionless parameter R_B as follows:

$$R_B = \frac{{u_*}^2}{\omega_p \upsilon_a} \tag{7}$$

Here, υ_a is the kinematic viscosity of air, and ω_p is the peak angular frequency of wind waves. The above dimensionless parameter can be regarded as the windsea Reynolds number, and it gives the critical condition for wave breaking. Therefore, R_B may be an important parameter to quantify the process of the ocean surface boundary and to describe the properties of whitecaps (see Zhao and Toba (2001)). It is natural to consider that there should be a high correlation between R_B and W_c_AWE or W_D_AWE. As shown in Fig.10, there is a linear relation between W_c_AWE and R_B, with a correlation coefficient of 0.6 as the linear regression, whereas the

relation of W_D_AWE with R_B has a higher correlation coefficient as 0.81, which shows that as the new physical quantity for evaluating ocean whitecaps W_D is more persuasive and expectable than whitecap coverage W_C.

5. CONCLUSIONS

In this study, the image data of the ocean surface obtained from a sea observation tower were digitally processed by the AWE and fixed threshold methods, and the average whitecap coverage over 20 minutes was calculated from 120 sea images. By comparing whitecap coverage calculated by AWE with that of fixed threshold method, the usefulness of AWE in long-term observation was examined. In the AWE algorithm assessment, we compared the solar radiation data with the whitecap coverage values during the observation period, and examined the relationship between them. The values of W_c_FT were in good agreement with the empirical relations for whitecap coverage by Monahan (1993) and Sugihara (2007). On the other hand, the values of W_c_AWE were larger than those from the empirical relations, but they were found to be consistent with the relation of Stramska and Petelski (2003). After selecting the effective data of whitecap coverage, it was shown that the correlation coefficient between Wc_AWE $^{1/3}$ and U_{10} was 0.76, whereas that between Wc_FT$^{1/3}$ and U_{10} was 0.88. According to these results, it was concluded that the AWE extraction of whitecaps has high accuracy, but the data obtained under the condition of strong light may be too large. In order to find out the reason for the difference in accuracy of each method, the difference between Wc_AWE and Wc_FT was verified, indicating that the value obtained by AWE's automatic detection algorithm becomes too large under the condition of strong light. In order to describe the physical characteristics of ocean whitecaps more accurately, we introduced a new three-dimensional physical quantity, i.e., whitecap depth W_D, and verified the relation between W_D and the windsea Reynolds number R_B. The present results demonstrated that W_D is in good correlation with R_B, and thus suggesting that whitecap depth is more suitable parameter than whitecap coverage, which is only two-dimensional information on whitecaps.

ACKNOWLEDGMENTS

This work was partially supported by a Grant-in-Aid for Scientific Research (B) (Coordinator: Y. Sugihara, JSPS KAKENHI Grant Number JP19H02249)

REFERENCES

Asher, W. E., J. Edson, W. R. McGillis, R. Wanninkhof, D. T. Ho and T. Litchendorf.(2002) Fractional area whitecap coverage and air-sea gas transfer velocities measured during GasEx-98. *Gas Transfer at Water Surfaces*., pp.199-203.,

Asher, W. E. and R. Wanninkhof.(1998) The effect of bubble-mediated gas transfer on purposeful dual-gaseous tracer experiments. *J. Geophys. Res*., Vol.103, pp.10555-10560.

Cardon, V. J.(1970) Specification of the wind distribution in the marine boundary layer for wave forecasting. *New York University, New York,* 131 pp.

Gathman, S. and E. M. Trent.(1968)Space charge over the open ocean. *J. Atmos. Sci*., Vol.25, pp.1075-1079.

Lewis, E. R. and Schwartz, S. E.(2004) *Sea Salt Aerosol Production. Mechanisms, Measurements, and Models*. Geophysical Monographs 152. American Geophysical Union, Washington, DC, 412 pp.

Munk, W. H.(1947) A critical wind speed for air-sea boundary process. *J. Marine res*., Vol.6, pp.203-218.

Monahan, E. C.(1971) Ocean whitecaps. *J. Phys. Oceanogr*., Vol.1, pp.139-144.

Monahan, E. C.(1993) Occurrence and evolution of acoustically relevant subsurface bubble plume and their associated, remotely monitorable surface whitecaps. Natural Sources of Underwater Sound, edited by B. R. Kerman, pp.503-517., Kluwer Acad., Norwell, Mass.

Monin, A . S. and A. M. Obukhov.(1954) The basic regularity in turbulent mixing in the surface layer. *Trudy Geofiz* Inst. Nauk, SSSR, Vol.24, pp.163-187.

Mizuno,Y.(2008) A study on quantification for whitecaps by using imaging measurement, *Thesis of Master degree*, Interdisciplinary Graduate School of Engineering Sciences, Kyushu University. (in Japanese)

Paulson, C. A.(1970) The mathematical representation of wind speed and temperature profiles in the unstable atmospheric surface layer, *J. Appl. Metior*., Vol.9, pp.857-861.

Ross, D. B. and V. Cardone.(1974) Observations of oceanic whitecaps and their relation to remote measurements of surface wind speed. *J. Geophys. Res*., Vol.79, pp.444-452.

Stramska, M. and T. Petelski.(2003) Observation of oceanic whitecaps in the north polar waters of the Atlantic. *J. Geophys. Res*., Vol.108, No.C3, 3086, doi:10.

Sugihara, Y., H. Tsumori, T. Ohga, H. Yoshioka and S. Serizawa.(2007) Variation of whitecap coverage with wave-field conditions. *J. Marine Res*., Vol.66, pp.47-60.

Thorpe, S. A. (1986). Measurements with an automatically recording inverted echo sounder; ARIES and the bubble clouds. *Journal of physical oceanography*, Vol.16, pp.1462-1478.

Toba, Y. and Chaen, M.(1973) Quantitative expression of the breaking of wind waves on the sea surface. *Rec. Oceanogr. Works Jpn*., 12 : 1-11.

Toba, Y. and M. Koga.(1986) A parameter describing overall conditions of wave breaking, whitecapping, sea-spray production and wind stress. *Oceanic Whitecaps*, pp.37-47.

Wannninkhof, R. H. and L. F. Bliven.(1991) Relationship between gas exchange, wind speed, and radar backscatter in a large wind-wave tank. *J. Geophys. Res.*, Vol.96, pp.2785-2795.

Wu, J.(1979) Oceanic whitecaps and sea state. *J. Phys. Ocesnogr.*, 16：2172-2178.

Wu, J.(1980) Wind-stress coefficients over sea surface near neutral conditions－A revisit. *J. Phys. Oceanogr.*, Vol.10, pp.727-740.

Yelland, M. and P. K. Taylor.(1996) Wind stress measurements from the open ocean. *J. Phys. Oceanogr.*, Vol.26, pp.541-558.

Yoshioka,H.(2003) Acoustically observed characteristics of bubble entrainment due to wave breaking. *Proceedings of coastal engineering,JSCE.* Vol.50, pp.116-120.

Zhao, D. and Y. Toba.(2001)Dependence of whitecap coverage on wind and wind-wave properties. J. Oceanogr., Vol.57, pp.603-616.